The Configurations $3s^2 3p^5 3d$ and $3s 3p^6 3d$ in Mn VIII and Fe IX

Physica Scripta. Vol. 27, 364–366, 1983

The Configurations $3s^2 3p^5 3d$ and $3s3p^6 3d$ in Mn VIII and Fe IX

Rikard Smitt and Lars Åke Svensson*

Department of Physics, University of Lund, Lund, Sweden

Received February 10, 1983; accepted February 25, 1983

Abstract

The astrophysically important configuration $3s^2 3p^5 3d$ has been determined for Mn VIII and Fe IX by means of about 60 lines, classified as combinations $3s^2 3p^6$–$3s^2 3p^5 3d$ and $3s^2 3p^5 3d$–$3s3p^6 3d$.

We also introduce a sensitive method for isoelectronic comparison of energy parameters. By this method the configuration $3s^2 3p^5 3d$ is studied through the Ar I sequence, thus supporting the reported Mn VIII and Fe IX identifications.

1. Introduction

A great interest has been attached to the configuration $3s^2 3p^5 3d$ in the Ar I sequence. In 1974 Svensson et al. [1] were able to propose identifications of 10 coronal lines with magnetic-dipole and electric-quadrupole transitions within this configuation in Fe IX and Ni XI. The identifications were made possible by laboratory studies of several spectra in the sequence. A few years earlier Wagner and House [2] had made an attempt to determine $3s^2 3p^5 3d$ by studying its combinations with $3s^2 3p^5 4f$ in the spectra from V VI to Fe IX. However, the data were insufficient to provide any definitive identifications of coronal lines.

At our laboratory we simultaneously studied spectra from Sc IV to Fe IX. The analyses of the spectra Sc IV to Cr VII [3–6] are quite comprehensive and contain several configurations. In this paper we discuss the results for Mn VIII and Fe IX. We have then concentrated our study on the transition $3s^2 3p^5 3d$–$3s3p^6 3d$, which provides the most favourable way of determining the levels of $3s^2 3p^5 3d$.

The manganese and iron spectra were recorded in our 3-m normal-incidence spectrograph. We used a gold replica grating from Bausch & Lomb with 1200 grooves mm^{-1}, which gives a plate factor of about 2.8 Å mm^{-1}. The light source was a triggered open spark operated at about 50 kV. The wavelength determination has been based on standard lines provided mainly from spectra of oxygen, iron and manganese. In the actual wavelength region (300–500 Å) a great number of resonance lines belonging to lower stages of ionization appear on the spectrograms. In some cases our measurements are strongly influenced by close-lying lines. Still we consider the errors of the experimentally determined levels to be less than 6 cm^{-1}.

2. $3s^2 3p^5 3d$ and $3s3p^6 3d$ in Mn VIII

The manganese spectrum has been measured on several spectrograms, the strongest lines both in the first and the second order. About 30 lines in the region between 320 and 420 Å have been classified as belonging to $3s^2 3p^5 3d$–$3s3p^6 3d$.

The energy relative to the ground state $3s^2 3p^6\ {}^1S_0$ has been determined from the three possible combinations with levels in $3s^2 3p^5 3d$, those with $J = 1$. The strongest one, ${}^1S_0$–${}^1P_1$ at 185.455 Å, has been measured in the second to the fourth order. ${}^1S_0$–${}^3D_1$ at 236.218 Å has been observed in the second and third order. The rather weak line ${}^1S_0$–${}^3P_1$ at 266.181 Å only appears in the first order. The wavenumber of this line deviates from the adopted level value of ${}^3P_1$ with about 20 cm^{-1}, which indicates a coincidence with another manganese line.

Around 400 Å several very strong Mn V lines appear, and it is difficult to resolve the Mn VIII spectrum in that region. This has caused an increased uncertainty in the determination of $3s^2 3p^5 3d\ {}^3D$ and ${}^1D$. However, these identifications are confirmed by the isoelectronic comparison of energy integrals, illustrated in Figure 1.

Most of the lines have been measured only in the first order, and we estimate the uncertainty of the wavelengths to be about 0.01 Å. The observed Mn VIII lines are given in Table I and the energy levels in Table III.

3. $3s^2 3p^5 3d$ and $3s3p^6 3d$ in Fe IX

The spectrum Fe IX has been measured in the first order. The study of the transition $3s^2 3p^5 3d$–$3s3p^6 3d$ has led to the classi-

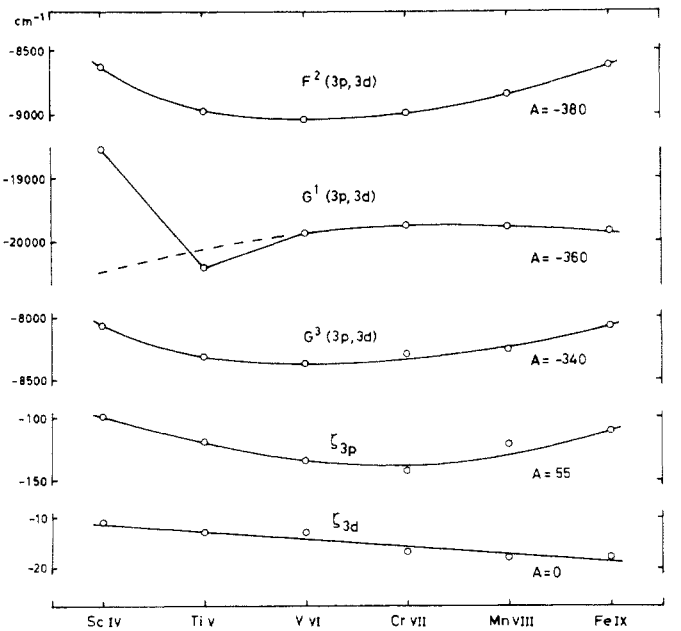

Fig. 1. Isoelectronic comparison of energy integrals belonging to $3s^2 3p^5 3d$. The plotted quantity is $\Delta E - A(Z-17)$, where ΔE is the difference between observed and theoretically calculated integral values, and A is fitted to make the curves approximately horizontal.

* Present address: Tetra Pak International AB, Lund, Sweden.

Table I. *Observed lines in Mn VIII*

Intensity	λ (Å)	σ(cm^{-1})	Combination
			$3s^2 3p^6 - 3s^2 3p^5 3d$
20	185.455	539 214	$^1S_0 - {}^1P_1$
15	236.218	423 338	$^1S_0 - {}^3D_1$
5[a]	266.181	375 684	$^1S_0 - {}^3P_1$
			$3s^2 3p^5 3d - 3s3p^6 3d$
1	323.782	308 850	$^3P_2 - {}^1D_2$
8	340.114	294 019	$^3P_0 - {}^3D_1$
0[b]	340.234	293 915	$^3F_3 - {}^1D_2$
10	341.770	292 594	$^3P_1 - {}^3D_2$
7	342.501	291 970	$^3P_1 - {}^3D_1$
3	344.493	290 282	$^3F_2 - {}^1D_2$
11	345.617	289 338	$^3P_2 - {}^3D_3$
8	346.842	288 316	$^3P_2 - {}^3D_2$
2	347.602	287 685	$^3P_2 - {}^3D_1$
11	360.373	277 490	$^3F_4 - {}^3D_3$
5	364.427	274 403	$^3F_3 - {}^3D_3$
10	365.779	273 389	$^3F_3 - {}^3D_2$
5	370.722	269 744	$^3F_2 - {}^3D_2$
6	371.090	269 476	$^3D_3 - {}^1D_2$
9	371.586	269 117	$^3F_2 - {}^3D_1$
8	371.695	269 038	$^1D_2 - {}^1D_2$
5	378.482	264 213	$^3D_2 - {}^1D_2$
9	382.666	261 324	$^1F_3 - {}^1D_2$
8	400.075	249 953	$^3D_3 - {}^3D_3$
3	400.781	249 513	$^1D_2 - {}^3D_3$
5[c]	402.446	248 481	$^1D_2 - {}^3D_2$
2[c]	403.497	247 833	$^1D_2 - {}^3D_1$
0[c]	408.206	244 974	$^3D_1 - {}^3D_2$
5[c]	408.685	244 687	$^3D_2 - {}^3D_3$
5[c]	409.270	244 337	$^3D_1 - {}^3D_1$
6[d]	410.374	243 680	$^3D_2 - {}^3D_2$
0	411.473	243 029	$^3D_2 - {}^3D_1$
5	413.582	241 790	$^1F_3 - {}^3D_3$
4[d]	415.348	240 762	$^1F_3 - {}^3D_2$
0	668.288	149 636	$^1P_1 - {}^1D_2$

[a] Possibly blend.
[b] Broad line. Possibly blend.
[c] Affected by a close-lying Mn V line.
[d] Blend with Mn V.

Table II. *Observed lines in Fe IX*

Intensity	λ (Å)	λ_{calc} (Å)	σ (cm^{-1})	Combination
				$3s^2 3p^6 - 3s^2 3p^5 3d$
120	171.073[a]		584 546	$^1S_0 - {}^1P_1$
10	217.100[a]		460 617	$^1S_0 - {}^3D_1$
5	218.935[a]		456 757	$^1S_0 - {}^3D_2$
30	241.739[a]		413 669	$^1S_0 - {}^3P_2$
20	244.911[a]		408 312	$^1S_0 - {}^3P_1$
				$3s^2 3p^5 3d - 3s3p^6 3d$
2	311.563	.563	320 962	$^3P_0 - {}^3D_1$
4	313.234	.239	319 250	$^3P_1 - {}^3D_2$
5	317.194	.193	315 264	$^3P_2 - {}^3D_3$
2	318.586	.582	313 887	$^3P_2 - {}^3D_2$
0	319.426	.423	313 062	$^3P_2 - {}^3D_1$
6	329.890	.897	303 131	$^3F_4 - {}^3D_3$
5	335.294	.290	298 246	$^3F_3 - {}^3D_2$
2	339.838	.842	294 258	$^3D_3 - {}^1D_2$
4	341.150	.159	293 126	$^1D_2 - {}^1D_2$
4	341.390	.396	292 920	$^3F_2 - {}^3D_1$
1	348.124	.123	287 254	$^3D_2 - {}^1D_2$
4	352.072	.060	284 033	$^1F_3 - {}^1D_2$
	masked by Fe V			$^3D_3 - {}^3D_3$
1	369.260	.266	270 812	$^1D_2 - {}^3D_2$
0	374.605	.610	266 948	$^3D_1 - {}^3D_2$
2	375.773	.773	266 118	$^3D_1 - {}^3D_1$
2	377.443	.439	264 941	$^3D_2 - {}^3D_2$
0	378.629	.620	264 111	$^3D_2 - {}^3D_1$
2	380.079	.074	263 103	$^1F_3 - {}^3D_3$
0	604.880	.869	165 322	$^1P_1 - {}^1D_2$

[a] Observed in the solar spectrum [7].

fication of about 20 lines between 310 Å to 380 Å. The energy relative to the ground level is given by the five combinations observed in the solar spectrum by Behring et al. [7]. Two of the lines, $^1S_0 - {}^3P_2$ and $^1S_0 - {}^1D_2$, originate from magnetic-quadrupole transitions, which are able to appear in the low-density solar plasma.

As in Mn VIII we estimate the uncertainty of the wavelengths to be about 0.01 Å. Most of the Fe IX levels, however, are more accurately connected by the coronal transitions within $3s^2 3p^5 3d$. The errors in the connection to the ground level are estimated to be less than 6 cm^{-1}.

The observed Fe IX lines are given in Table II and the energy levels in Table III. For $3s^2 3p^5 3d$ we have adopted the level values from Edlén and Smitt [8].

4. Calculations and isoelectronic studies

According to Slater the energy matrix of $3s^2 3p^5 3d$ contains the electrostatic integrals E_{av}, $F^2(3p, 3d)$, $G^1(3p, 3d)$, $G^3(3p, 3d)$ and the spin-orbit integrals ζ_{3p} and ζ_{3d}. In our parametric calculations we also introduced the effective electrostatic integrals $D^1(3p, 3d)$ and $X^2(3p, 3d)$ as defined by Goldschmidt [9]. The integrals were determined by least-squares fits to the observed levels. The resulting integral values are given in Table IV together with the corresponding Hartree–Fock (HF) values. The resulting energy levels of $3s^2 3p^5 3d$ and the percentage composition of the eigenvectors in *LS*-coupling are given in Table V. Eigenvector components of less than 5% have been excluded.

In order to check the validity of the identifications we introduce a sensitive method for isoelectronic studies similar to the one described in [8]. The difference between the fitted parameter value and the Hartree–Fock value is determined and then, after subtracting the linear part of its Z-dependence, plotted against Z. A comparison of the $3s^2 3p^5 3d$ integrals in

Table III. *Energy levels (in cm^{-1}) of Mn VIII and Fe IX*

Level		Mn VIII	Fe IX[a]
$3s^2 3p^5 3d$	$^3P_0$	373 658	405 772
	$^3P_1$	375 710	408 315.1
	$^3P_2$	379 993	413 669.2
	$^3F_4$	391 836	425 809.8
	$^3F_3$	394 921	429 310.9
	$^3F_2$	398 564	433 818.8
	$^3D_3$	419 374	455 616.2
	$^1D_2$	419 817	456 752.7
	$^3D_1$	423 337	460 616
	$^3D_2$	424 641	462 616.6
	$^1F_3$	427 531	465 828.4
	$^1P_1$	539 214	584 546
$3s3p^6 3d$	$^3D_1$	667 677	726 734
	$^3D_2$	668 308	727 560
	$^3D_3$	669 326	728 935
	$^1D_2$	688 850	749 871

[a] Energy levels from [8].

Table IV. *Energy parameters (in cm^{-1}) for $3s^23p^53d$ and $3s3p^63d$*

Ion	Parameter	HF-value	Fitted	Fitted/HF
Mn VIII	$3s^23p^53d$			
	E_{av}	406 129	412 049 ± 11	1.015
	$F^2(3p, 3d)$	119 370	107 484 ± 95	0.900
	$G^1(3p, 3d)$	143 091	120 423 ± 32	0.842
	$G^3(3p, 3d)$	90 300	79 322 ± 168	0.878
	ζ_{3p}	7599	7917 ± 33	1.042
	ζ_{3d}	594	576 ± 12	0.970
	$D^1(3p, 3d)$		3793 ± 82	
	$X^2(3p, 3d)$		4977 ± 157	
Mean error of the least-squares level fit ± 35 cm^{-1}				
	$3s3p^63d$			
	E_{av}	716 284	673 705 ± 1	0.941
	$G^2(3s, 3d)$	111 035	50 377 ± 8	0.454
	ζ_{3d}	595	659 ± 1	1.108
Mean error of the least-squares level fit ± 2 cm^{-1}				
Fe IX	$3s^23p^53d$			
	E_{av}	440 542	448 137 ± 16	1.017
	$F^2(3p, 3d)$	128 434	116 392 ± 143	0.906
	$G^1(3p, 3d)$	152 397	129 299 ± 47	0.848
	$G^3(3p, 3d)$	96 768	85 638 ± 259	0.885
	ζ_{3p}	9533	9917 ± 48	1.040
	ζ_{3d}	802	784 ± 18	0.978
	$D^1(3p, 3d)$		4013 ± 121	
	$X^2(3p, 3d)$		5254 ± 245	
Mean error of the least-squares level fit ± 51 cm^{-1}				
	$3s3p^63d$			
	E_{av}	774 597	733 497 ± 2	0.947
	$G^2(3s, 3d)$	117 958	54 406 ± 14	0.461
	ζ_{3d}	802	880 ± 3	1.097
Mean error of the least-squares level fit ± 3 cm^{-1}				

Table V. *Calculated level values (in cm^{-1}) of $3s^23p^53d$*

	J	E_{calc}	$E_{obs}-E_{calc}$	Percentage composition
Mn VIII	0	373 619	39	100 ^3P
	1	375 725	−15	99 ^3P
		423 357	−20	99 ^3D
		539 214	0	100 ^1P
	2	380 018	−25	98 ^3P
		398 552	12	95 ^3F
		419 828	−11	73 ^1D + 22 ^3D + 5 ^3F
		424 606	35	75 ^3D + 23 ^1D
	3	394 941	−20	96 ^3F
		419 379	−5	71 ^3D + 29 ^1F
		427 528	3	69 ^1F + 27 ^3D
	4	391 828	8	100 ^3F
Fe IX	0	405 712	60	100 ^3P
	1	408 340	−25	99 ^3P
		460 640	−24	99 ^3D
		584 546	0	100 ^1P
	2	413 706	−37	98 ^3P
		433 802	17	92 ^3F
		456 770	−17	70 ^1D + 23 ^3D + 7 ^3F
		462 571	46	72 ^3D + 25 ^1D
	3	429 343	−32	94 ^3F
		455 625	−9	69 ^3D + 31 ^1F
		465 822	6	66 ^1F + 29 ^3D + 6 ^3F
	4	425 795	15	100 ^3F

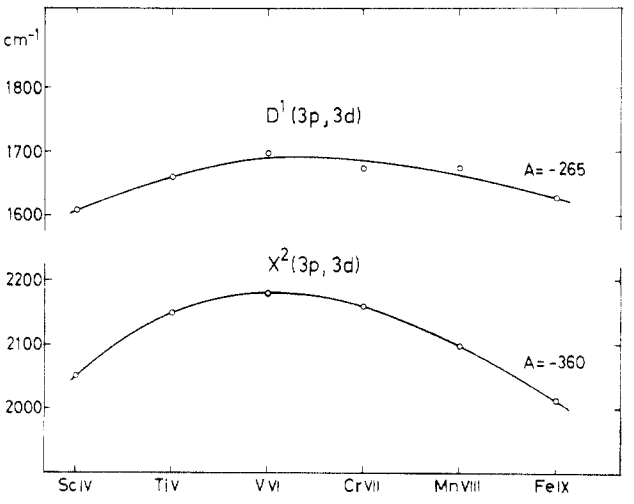

Fig. 2. Isoelectronic comparison of the effective electrostatic integrals D^1 and X^2 in $3s^23p^53d$. Before plotting we have subtracted $A(Z-17)$ from the integral values. See text to Fig. 1.

the Ar I sequence is shown in Fig. 1. The small deviations from the curves of F^2, G^3, ζ_{3p} and ζ_{3d} can be fully explained by possible experimental errors. In the case of G^1 the deviations from the dotted curve in Sc IV and Ti V arise from the strong interaction between $3s^23p^53d\ ^1P_1$ and $4s\ ^1P_1, ^3P_1$ in these two spectra.

Since no HF-values were available for the effective electrostatic parameters D^1 and X^2, we have chosen to illustrate the behavior of these two parameters in the sequence merely by subtracting the linear parts of their Z-dependence before plotting. This is shown in Fig. 2. As the parameters are relatively small (and, in this sequence obviously almost linear in Z) the curves are very sensitive to changes of the level values.

This method provides a reliable way of determining energy levels in highly ionized atoms and may be helpful in analyzing spectra of high-temperature plasmas. Studies of such spectra are frequently based on ab initio calculations of energy levels. However, by extrapolating curves of the kind described above, we can obtain more accurate predictions of levels, which will extend our knowledge of spectra in astrophysical and laboratory plasmas.

Acknowledgement

We wish to thank Prof. Bengt Edlén who has supported us with valuable advice during this investigation. The work has been supported by the Swedish Natural Science Research Council (NFR), and the National Board for Energy Source Development (NE).

References

1. Svensson, L. Å., Ekberg, J. O. and Edlén, B., Solar Physics **34**, 173 (1974).
2. Wagner, W. J. and House, L. L., Astrophys. J. **166**, 683 (1971).
3. Smitt, R., Physica Scripta **8**, 292 (1973).
4. Svensson, L. Å., Physica Scripta **13**, 235 (1976).
5. Ekberg, J. O., Physica Scripta **13**, 111 (1976).
6. Ekberg, J. O., Physica Scripta **13**, 245 (1976).
7. Behring, W. E., Cohen, L., Feldman, U. and Doschek, G. A., Astrophys. J. **203**, 521 (1976).
8. Edlén, B. and Smitt, R., Solar Physics **57**, 239 (1978).
9. Goldschmidt, Z. B., J. Physics **B3**, L141 (1970).